A Closer Look at Tip-Enhanced Raman Chemical Reaction Nano-Images

Brian T. O'Callahan,* Patrick Z. El-Khoury*

[1]Earth and Biological Sciences Division, Pacific Northwest National Laboratory, P.O. Box 999, Richland, WA 99352, USA; [2]Physical Sciences Division, Pacific Northwest National Laboratory, P.O. Box 999, Richland, WA 99352, USA

*brian.ocallahan@pnnl.gov, *patrick.elkhoury@pnnl.gov

Abstract

Tip-enhanced Raman spectroscopy (TERS) is a powerful technique that enables ultrahigh spatial resolution and ultrasensitive chemical imaging. This technique's ability to track plasmon-induced/enhanced chemical reactions in real space has gained increasing popularity in recent years. In this study, we expose inherent difficulties associated with assigning TERS signatures that accompany chemical transformations. Namely, distinct selection rules as well as the possibility of multiple physical processes/chemical reaction pathways complicate spectral assignments and necessitate caution in assigning the experimental observables. We illustrate the latter using 4,4'-dimercaptostilbene functionalized plasmonic silver nanocubes, wherein we identify the TERS signatures of product formation, molecular charging, multipolar Raman scattering, and preferred molecular orientations that all lead to distinct and assignable spectral patterns.

Raman spectroscopy is a versatile chemical identification technique that has widely been used in the chemical, biological and material sciences. Despite its rich information content, the relatively small Raman scattering cross-sections of small and medium sized (bio)molecules is limiting. This led to the development of several approaches to enhance the Raman scattering from (bio)molecular and (bio)material systems. Tip-enhanced Raman scattering (TERS)[1] is one example of such approaches, wherein Raman scattering of molecules is amplified by locally enhanced optical fields at the apex of a plasmonic scanning probe tip. Down to single molecule sensitivity has been demonstrated using TERS, which is particularly evident in measurements performed at ultralow temperatures and ultrahigh vacuum.[2-6] Indeed, single molecules can be simultaneously imaged and fingerprinted with sub-molecular resolution in this regime.[3]

As highlighted in recent analyses from our group, the information content in TERS is rich with a number of physical and chemical processes contributing to the recorded spectral nano-images, particularly under ambient laboratory conditions.[7, 8] These include multipolar Raman scattering, molecular charging, Stark tuning, and molecular reorientation dynamics.[9-12] In this work, we show that these observations are general, and in the case of 4,4'-dimercaptostilbene (DMS) functionalized plasmonic silver nanocubes complicate the assignments of both parent (trans-DMS) as well as product (cis-DMS) spectra that we encounter throughout the course of TERS chemical reaction imaging. Through a rigorous analysis of TERS spectra contained within our recorded hyperspectral Raman nano-images, we stress that caution needs to be exercised in the assignments of peaks and spectral patterns that are often casually associated with plasmon-induced chemical changes.

We start our discussion with the most abundant TERS spectrum that we observe throughout the course of spectral nano-imaging. The TERS spectrum shown in Figures 1A and 1B is obtained by spatio-temporal averaging the nano-optical response that was optimally enhanced towards the

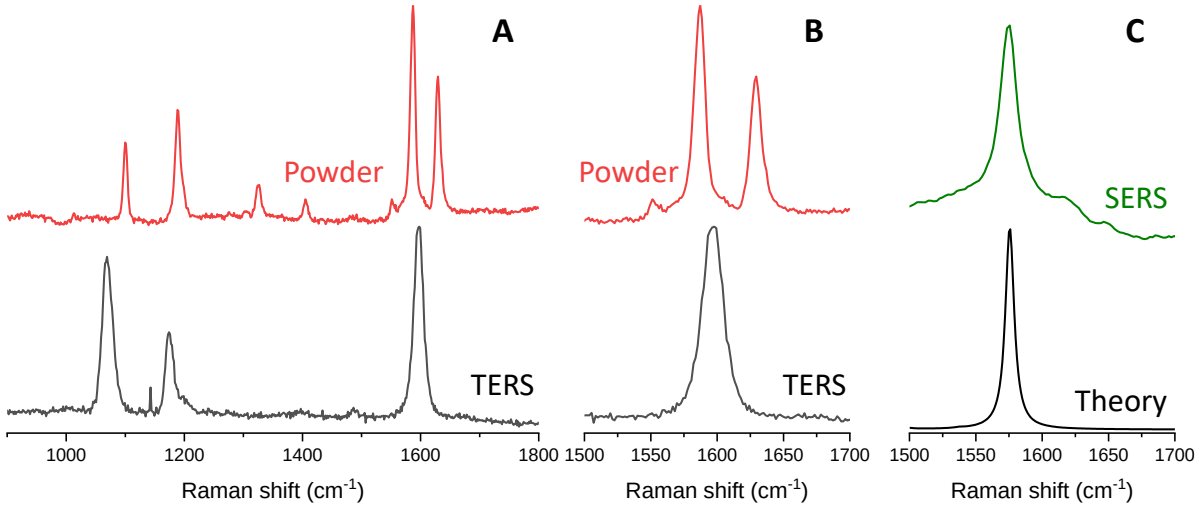

Figure 1. The Raman spectrum of the powder is compared to the spatio-temporally averaged TERS spectrum in A. Panel B highlights the 1500-1700 region of the spectrum, where the disappearance of the vinyl C=C stretching vibration is observed. Previous SERS spectra and a theoretical treatment that accounts for the orientation of trans-DMS molecules at a plasmonic junction are shown in C. See text for more details.

edges of plasmonic silver nanocubes, as shown in the supporting information section and previous studies.[7, 8] A quick comparison between the conventional Raman spectrum of trans-DMS crystals and the average TERS response reveals distinct relative intensities in the < 1200 cm^{-1} region of the

spectrum, as well as the absence of the vinyl signature (~1630 cm^{-1}) in the plasmon-enhanced spectrum. Similar spectral features were previously observed in ultrasensitive surface-enhanced Raman measurements[13] (also see Figure 1C) that interrogated trans-DMS molecules at plasmonic nanojunctions formed between plasmonic silver nanoparticles. These distinct spectral features

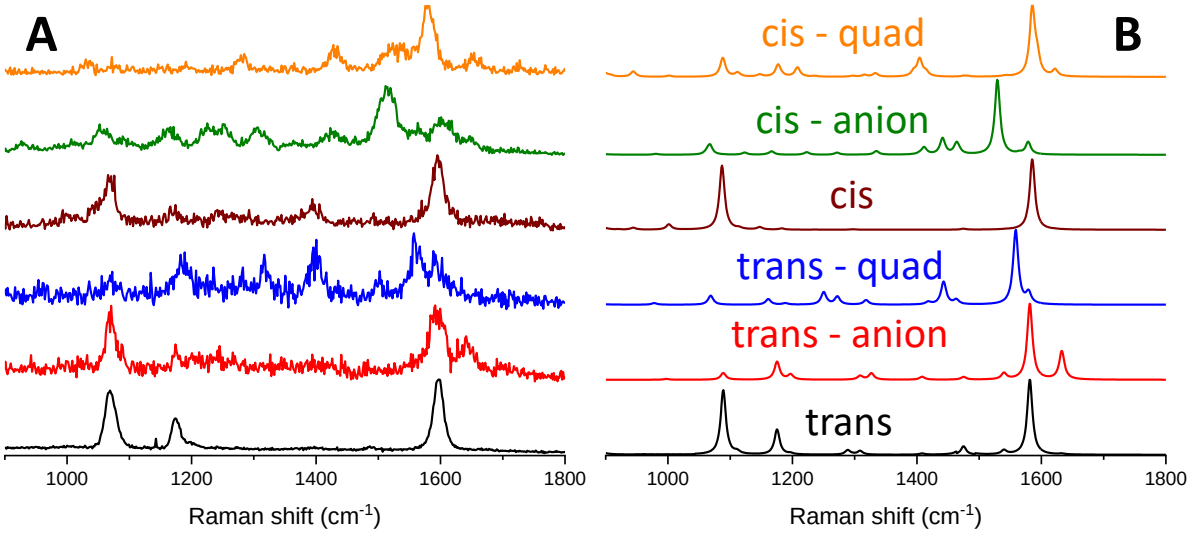

Figure 2. Selected spectra taken from the hyperspectral image cube represented in Figure S1. Both trans- as well cis- are captured throughout the course of TERS mapping. The forms are marked by their conventional dipolar (trans and cis labels) as well as quadrupolar or electric dipole-electric quadrupole (trans – quad and cis-quad) Raman spectra. We also observe spectra that can be assigned to the radical anions of both forms (marked by trans-anion and cis-anion). Both the relative shifts as well as the relative intensities of the observable states are well reproduced when experiment (panel A) is compared to theory (panel B). Note that orientationally averaged spectra are shown for all but the trans-DMS form (black trace).

were increasingly evident in the limit of a single (or a few) molecules. Indeed, the tensorial nature of Raman scattering governs spectra in this ultrasensitive regime,[14] as confirmed through simulations that account for a preferred molecular orientation relative to an anisotropic/unidirectional plasmonic field at plasmonic nanojunctions.[13] Given the extreme confinement of the optical field in the vicinity of the silver nanocube (~1-2 nm),[7, 8] the optical response is likely also governed by tensorial Raman scattering. Alternatively, the spatio-temporally averaged response in this work broadcasts the preferred orientation of trans-DMS on Ag. In both cases, the disappearance of a peak, herein the vinyl stretching vibration at ~1630 cm^{-1}, is not the result of chemical transformation. Rather, the removal of orientational averaging of trans-DMS molecules can give rise to the distinct TERS spectrum shown in Figure 1. As illustrated in the ensuing discussion, several other possibilities that lead to the disappearance of the same band can also be envisioned, which necessitates a more careful analysis of the spectral pattern as a whole as opposed to a single peak to faithfully assign our observables.

The above analysis of spatio-temporally averaged signals masks significant pixel to pixel variations in the recorded nano-optical response. A collection of single pixel TERS spectra is shown in Figure 2A. Together, these spectra paint a picture of the complex physical and chemical processes that together contribute to the recorded hyperspectral nano-image. Overall, significant differences in relative intensities are observed and molecular orientation alone cannot account for the observed spectral patterns. We therefore rely on density functional theory calculations guided by prior analyses of TERS spectral images of simpler aromatic thiols to assign our major

observables.[7, 8] Beside the signatures of oriented trans-DMS molecules that we discussed above (black experimental/theoretical plots in Figure 2A/2B), we also observe the radical anion of the same form (red plots). The latter supports recent assignments of TERS spectra recorded from 4-nitrothiophenol to plasmon-induced molecular charging.[10] Unfortunately, our measurements do not allow us to comment on the exact mechanism of electron transfer (direct *vs* hot). As discussed below, this would require ultrafast TERS measurements that – to the best of our knowledge - have not been performed to date.

The large optical field gradients that are operative in the TERS configuration also lead to the observation of higher-order Raman scattering.[9] The spectrum shown in blue (Figure 2) is well-matched to experimental and theoretical quadrupolar Raman scattering spectra of trans-DMS. The theoretical spectrum tracks the square of the electric dipole-electric quadrupole polarizability (A)[9, 15]

$$A_{\alpha\beta\gamma} = 2\sum_{n\neq 0} \omega_{n0} \frac{Re[\langle 0|\mu_\alpha|n\rangle\langle n|\Theta_{\beta\gamma}|0\rangle]}{{\omega_{n0}}^2 - \omega^2}$$

where ω is the incident light frequency, ω_{n0} is the energy difference of the ground and nth excited states, and μ and Θ are the electric dipole and electric quadrupole operators, respectively. The indices $\alpha\beta\gamma$ denote distinct elements of the third rank tensor. Several prior reports associated spectra observed at plasmonic nanojunctions with multipolar Raman scattering.[16-19] These works suggest that the ratio of field to field gradient has to be ~1 Å for the field gradient term to be comparable to the non-resonant plasmon-enhanced Raman field term. This requirement is satisfied using the platform and geometry used in this work, as recently illustrated for a simpler aromatic thiol.[9]

We also observe the cis isomer form of DMS, marked through its conventional dipolar (brown spectra in Figure 2A and B) and also quadrupolar (orange spectra) TERS signatures. Akin to the trans isomer, we also observe spectra than can be uniquely assigned to the anionic form of cis-DMS (dark green spectra). The exact mechanism of trans-cis isomerization under our current experimental conditions are very difficult to establish. Some possibilities include:

(i) Direct excited state isomerization under visible light irradiation as a result of modified ground/excited state energies and topographies at plasmonic junctions
(ii) Photoelectrochemical isomerization mediated by anions, which we clearly observe for both isomers
(iii) Thermal isomerization, with heat provided from hot carrier decay

The above mechanisms may also be affected by (i) large rectified local optical fields that are operative under our current experimental conditions,[7, 20] and (ii) mechanical/electrostatic effects arising from the tip that is in direct contact with the molecules. Based on our current results alone, it is difficult to establish which mechanism(s) lead to product formation herein.

Each of our observed spectra can potentially provide hints about the local plasmonic fields that both enhance molecular scattering cross-sections and lead to various chemical reactions at plasmonic tip-sample nanojunctions. Spatio-temporal field gradients aside, time resolved measurements are indeed needed to dissect at which stage of plasmonic decay the various product forms.[21] Indeed, observations of ultrafast (few-10's of femtosecond) product formation would implicate direct energy/electron transfer, whereas slower product formation (tens of picoseconds or longer) would likely be heat driven. The timescale of formation of the anionic species themselves can also reveal whether direct electron transfer or hot electrons lead to molecular charging at plasmonic nanojunctions. Even though answering these questions requires further

investigation, our present work clearly establishes that DMS is an ideal molecular reporter that may be used to disentangle complex plasmon-induced chemical changes on the nanoscale.

Methods

Bulk Raman spectra of DMS (powder, Sigma-Aldrich) were recorded using a commercial confocal micro-Raman system (LabRam HR Evolution, Horiba). Spectra were recorded using a 632.8 nm laser source focused onto the BTP crystals using a 100X (NA=0.95) air objective.

The TERS sample was prepared by first depositing a 10 μL stock solution of 75 nm silver nanocubes (nanoComposix) onto silicon chip. After the drop was air dried, the substrate was rinsed with 5 mL of ethanol. Subsequently, 20 μL of 1 mM ethanolic solution of DMS was deposited onto the dispersed nanoparticles. Excess/unbound DMS molecules were washed off using ample amounts of ethanol, and the final sample was dried using a stream of dry nitrogen.

Our TERS setup is described elsewhere in more detail.[22] For the purpose of this work, as-purchased silicon probes (Nanosensors, ATEC) were coated with 75 nm of Ag and used for AFM (tapping mode feedback) and TER (SpecTop, Horriba Scientific) topographic/chemical imaging. For the latter, TERS signals were collected when the tip is in direct contact with the surface. A semi-contact mode is otherwise used to move the sample relative to the tip (pixel to pixel). For TERS measurements, a 633 nm diode laser (~150 μW) is focused onto the tip apex at a ~65º angle with respect to the surface normal using a 100 X air objective (Mitutoyo, 0.7 NA). The polarization of the laser was set to coincide with the tip axis using a half-waveplate. The back-scattered light was collected using the same objective, filtered through a series of long pass/dichroic filters, and recorded using a CCD camera (Andor, Newton EMCCD) coupled to a spectrometer (Andor, Shamrock 500) equipped with a 300 l/mm grating blazed at 550 nm.

The theoretical spectra presented in this work were obtained using previously outlined procedures.[9, 13] All calculations presented here were otherwise performed using the PBE functional[23] with the def_2-TZVP basis set.[24]

AUTHOR INFORMATION

Corresponding Authors

*brian.ocallahan@pnnl.gov, *patrick.elkhoury@pnnl.gov

Data Availability

The data that support the findings of this study are available from the corresponding authors upon reasonable request.

Supplementary Material

Correlated AFM-TERS nano-images of DMS-coated nanocubes.

ACKNOWLEDGEMENT

PZE acknowledges support from the United States Department of Energy, Office of Science, Office of Basic Energy Sciences, Division of Chemical Sciences, Geosciences & Biosciences. BTO was supported by the United States Department of Energy, Office of Science, Office of

Biological and Environmental Research, through the bioimaging technology development program.

References

1. Stöckle, R. M.; Suh, Y. D.; Deckert, V.; Zenobi, R., Nanoscale chemical analysis by tip-enhanced Raman spectroscopy. *Chemical Physics Letters* **2000,** *318* (1), 131-136.
2. Zhang, R.; Zhang, Y.; Dong, Z. C.; Jiang, S.; Zhang, C.; Chen, L. G.; Zhang, L.; Liao, Y.; Aizpurua, J.; Luo, Y.; Yang, J. L.; Hou, J. G., Chemical mapping of a single molecule by plasmon-enhanced Raman scattering. *Nature* **2013,** *498* (7452), 82-86.
3. Lee, J.; Crampton, K. T.; Tallarida, N.; Apkarian, V. A., Visualizing vibrational normal modes of a single molecule with atomically confined light. *Nature* **2019,** *568* (7750), 78-82.
4. Li, L.; Schultz, J. F.; Mahapatra, S.; Liu, X.; Shaw, C.; Zhang, X.; Hersam, M. C.; Jiang, N., Angstrom-Scale Spectroscopic Visualization of Interfacial Interactions in an Organic/Borophene Vertical Heterostructure. *Journal of the American Chemical Society* **2021,** *143* (38), 15624-15634.
5. Jaculbia, R. B.; Imada, H.; Miwa, K.; Iwasa, T.; Takenaka, M.; Yang, B.; Kazuma, E.; Hayazawa, N.; Taketsugu, T.; Kim, Y., Single-molecule resonance Raman effect in a plasmonic nanocavity. *Nature Nanotechnology* **2020,** *15* (2), 105-110.
6. Park, K.-D.; Muller, E. A.; Kravtsov, V.; Sass, P. M.; Dreyer, J.; Atkin, J. M.; Raschke, M. B., Variable-Temperature Tip-Enhanced Raman Spectroscopy of Single-Molecule Fluctuations and Dynamics. *Nano Letters* **2016,** *16* (1), 479-487.
7. El-Khoury, P. Z.; Schultz, Z. D., From SERS to TERS and Beyond: Molecules as Probes of Nanoscopic Optical Fields. *The Journal of Physical Chemistry C* **2020,** *124* (50), 27267-27275.
8. El-Khoury, P. Z., Tip-Enhanced Raman Scattering on Both Sides of the Schrödinger Equation. *Accounts of Chemical Research* **2021,** *54* (24), 4576-4583.
9. Wang, C.-F.; Cheng, Z.; O'Callahan, B. T.; Crampton, K. T.; Jones, M. R.; El-Khoury, P. Z., Tip-Enhanced Multipolar Raman Scattering. *The Journal of Physical Chemistry Letters* **2020,** *11* (7), 2464-2469.
10. Wang, C.-F.; O'Callahan, B. T.; Kurouski, D.; Krayev, A.; El-Khoury, P. Z., The Prevalence of Anions at Plasmonic Nanojunctions: A Closer Look at p-Nitrothiophenol. *The Journal of Physical Chemistry Letters* **2020,** *11* (10), 3809-3814.
11. Gabel, M.; O'Callahan, B. T.; Groome, C.; Wang, C.-F.; Ragan, R.; Gu, Y.; El-Khoury, P. Z., Mapping Molecular Adsorption Configurations with <5 nm Spatial Resolution through Ambient Tip-Enhanced Raman Imaging. *The Journal of Physical Chemistry Letters* **2021,** *12* (14), 3586-3590.
12. Bhattarai, A.; Crampton, K. T.; Joly, A. G.; Wang, C.-F.; Schultz, Z. D.; El-Khoury, P. Z., A Closer Look at Corrugated Au Tips. *The Journal of Physical Chemistry Letters* **2020,** *11* (5), 1915-1920.
13. El-Khoury, P. Z.; Johnson, G. E.; Novikova, I. V.; Gong, Y.; Joly, A. G.; Evans, J. E.; Zamkov, M.; Laskin, J.; Hess, W. P., Enhanced Raman scattering from aromatic dithiols electrosprayed into plasmonic nanojunctions. *Faraday Discussions* **2015,** *184* (0), 339-357.
14. Banik, M.; El-Khoury, P. Z.; Nag, A.; Rodriguez-Perez, A.; Guarrottxena, N.; Bazan, G. C.; Apkarian, V. A., Surface-Enhanced Raman Trajectories on a Nano-Dumbbell: Transition from Field to Charge Transfer Plasmons as the Spheres Fuse. *ACS Nano* **2012,** *6* (11), 10343-10354.
15. Ruud, K.; Helgaker, T.; Bouř, P., Gauge-Origin Independent Density-Functional Theory Calculations of Vibrational Raman Optical Activity. *The Journal of Physical Chemistry A* **2002,** *106* (32), 7448-7455.

16. Moskovits, M.; DiLella, D. P., Intense quadrupole transitions in the spectra of molecules near metal surfaces. *The Journal of Chemical Physics* **1982,** *77* (4), 1655-1660.
17. Sass, J. K.; Neff, H.; Moskovits, M.; Holloway, S., Electric field gradient effects on the spectroscopy of adsorbed molecules. *The Journal of Physical Chemistry* **1981,** *85* (6), 621-623.
18. Polubotko, A. M., Manifestation of strong quadrupole light–molecule interaction in the SER and SEHR spectra of pyrazine and phenazine. *Chemical Physics Letters* **2012,** *519-520*, 110-117.
19. Aikens, C. M.; Madison, L. R.; Schatz, G. C., The effect of field gradient on SERS. *Nature Photonics* **2013,** *7* (7), 508-510.
20. Li, Z.; Rigor, J.; Large, N.; El-Khoury, P. Z.; Kurouski, D., Underlying Mechanisms of Hot Carrier-Driven Reactivity on Bimetallic Nanostructures. *The Journal of Physical Chemistry C* **2021,** *125* (4), 2492-2501.
21. Warkentin, C. L.; Yu, Z.; Sarkar, A.; Frontiera, R. R., Decoding Chemical and Physical Processes Driving Plasmonic Photocatalysis Using Surface-Enhanced Raman Spectroscopies. *Accounts of Chemical Research* **2021,** *54* (10), 2457-2466.
22. El-Khoury, P. Z.; Aprà, E., Spatially Resolved Mapping of Three-Dimensional Molecular Orientations with ∼2 nm Spatial Resolution through Tip-Enhanced Raman Scattering. *The Journal of Physical Chemistry C* **2020,** *124* (31), 17211-17217.
23. Perdew, J. P.; Burke, K.; Ernzerhof, M., Generalized Gradient Approximation Made Simple. *Physical Review Letters* **1996,** *77* (18), 3865-3868.
24. Weigend, F.; Ahlrichs, R., Balanced basis sets of split valence, triple zeta valence and quadruple zeta valence quality for H to Rn: Design and assessment of accuracy. *Physical Chemistry Chemical Physics* **2005,** *7* (18), 3297-3305.